ISSN 1063-7761, Journal of Experimental and Theoretical Physics, 2008, Vol. 106, No. 6, pp. 1109–1117. © Pleiades Publishing, Inc., 2008.
Original Russian Text © V.S. Zhandun, N.G. Zamkova, V.I. Zinenko, 2008, published in Zhurnal Éksperimental'noĭ i Teoreticheskoĭ Fiziki, 2008, Vol. 133, No. 6, pp. 1266–1276.

ORDER, DISORDER, AND PHASE TRANSITION IN CONDENSED SYSTEMS

Lattice Dynamics, Ferroelectric and Antiferroeelctric Instabilities, and the Ferroelectric Phase Transition in Disordered $PbB'_{1/2}B''_{1/2}O_3$ (B' = Ga, In, Lu; B'' = Nb, Ta) Solid Solutions

V. S. Zhandun*, N. G. Zamkova, and V. I. Zinenko

Kirensky Institute of Physics, Siberian Branch, Russian Academy of Sciences, Krasnoyarsk, 660036 Russia

**e-mail: jvc@iph.krasn.ru*

Received December 11, 2007

Abstract—The lattice vibration spectra, rf permittivity, and dynamic Born charges of disordered $PbB'_{1/2}B''_{1/2}O_3$ (B' = Ga, In, Lu; B'' = Nb, Ta) solid solutions are calculated in terms of the generalized Gordon–Kim model. All the compounds are found to have soft modes related to the center (Γ_{15}) and boundary point R (R_{15}) of the Brillouin zone; the frequencies of these modes are close. The ferroelectric phase transition temperatures and the spontaneous polarization in the ferroelectric phase are calculated for the solid solutions using a model Hamiltonian in the local mode approximation and the Monte Carlo method. These temperatures for the tantalum compounds are found to be higher than for the niobium compounds, and temperature t_s increases with the atomic number of ion B'. A model where the antiferroelectric state is related to the condensation of modes Γ_{15} and R_{15} is proposed. It is found that, for all compounds except for $PbSc_{1/2}Nb_{1/2}O_3$ and $PbSc_{1/2}Ta_{1/2}O_3$, the ferroelectric phase, which is only related to the condensation of mode R_{15}, and the antiferroelectric phase have similar energies. In $PbIn_{1/2}Ta_{1/2}O_3$, the antiferroelectric phase turns out to be energetically favorable.

PACS numbers: 63.20.-e, 77.80.-e

DOI: 10.1134/S1063776108060101

1. INTRODUCTION

Complex ABO_3 oxides have been extensively studied for more than 50 years. Interest in these compounds has recently quickened due to new possibilities of their practical application [1]. Lead-containing $PbB'_{1/2}B''_{1/2}O_3$ (B' = Sc, Ga, In, Lu; B'' = Nb, Ta) solid solutions are of particular interest from a practical viewpoint. The high-temperature phase of the B-cation-disordered $PbB'_{1/2}B''_{1/2}O_3$ compounds has cubic symmetry $Pm3m$. As the temperature decreases, these compounds undergo various sequences of phase transitions, including ferroelectric and antiferroelectric transitions, and the symmetry of the low-temperature phases and the sequence and character of the phase transitions depend on the chemical composition and ordering of cations B' and B''.

The compositions where B' = Sc, namely, $PbSc_{1/2}Nb_{1/2}O_3$ (PSN) and $PbSc_{1/2}Ta_{1/2}O_3$ (PST), have received the most study. Both solid solutions undergo a ferroelectric phase transition into an $R3$ rhombohedral phase, and this transition in fully ordered Pb_2ScNbO_6 and Pb_2ScTaO_6 compounds is sharp. As the degree of Sc and Nb(Ta) disordering increases, this transition is smeared, and the compounds begin to exhibit relaxor properties. However, the authors of [2, 3] noted that more detailed structural studies revealed locally ordered (in B cations) nanoregions with an antiferroelectric state in PST. There also exist certain experimental indications of antiferroelectric phase transitions in solid solutions with a heavier B' ion, such as $PbIn_{1/2}B''_{1/2}O_3$ (PIN, PIT) and $PbLu_{1/2}B''_{1/2}O_3$ (PLN, PLT) [4]. However, in contrast to PSN and PST, the $PbB'_{1/2}Nb_{1/2}O_3$ and $PbB'_{1/2}Ta_{1/2}O_3$ (B' = Ga, In, Lu) compounds are poorly understood, and attention has been mainly focused on PIN [1, 5–9].

Moreover, these compounds are interesting due to the fact that, as ion B' becomes heavier (from Sc to Lu), the ferroelectric phase transition in them is likely to change into an antiferroelectric transition [10], and transitions between the antiferroelectric and ferroelectric phases become possible. The mechanisms of these transitions are still incompletely clear from both theoretical and experimental viewpoints.

The purpose of this work is to calculate lattice vibration spectra, the ferroelectric phase transition temperatures, and the spontaneous polarizations and energies of the phases with ferroelectric and antiferroelectric dis-

Table 1. Experimental (a_{exp}) and calculated equilibrium (a_{min}) unit cell parameters

	a_{min}, Å	a_{exp}, Å		a_{min}, Å	a_{exp}, Å
PSN	3.94	4.07 [15]	PST	3.99	4.07 [16]
PGN	3.98	–	PGT	4.04	–
PIN	4.04	4.11 [17]	PIT	4.07 [10]	4.08 [17]
PLN	4.09	–	PLT	4.12	–

tortions for the series of fully disordered $Pb(B'_{1/2}B'')_{1/2}O_3$ (B' = Sc, Ga, In, Lu; B'' = Nb, Ta) solid solutions. The lattice dynamics and the ferroelectric phase transition for the scandium solid solutions were calculated in [11, 12]. In this work, we give some results of this calculation to complement this series of compounds.

In Section 2, we present the procedure and results of the calculation of the lattice dynamics of the disordered solid solutions. In Section 3, we discuss the results of the Monte Carlo simulation of the ferroelectric transition temperatures and the temperature dependences of the spontaneous polarizations of the compounds under study using an effective Hamiltonian. In Section 4, we consider a model for an antiferroelectric instability in the solid solutions, calculate the energy of a model antiferroelectric structure forming upon the condensation of the Γ_{15} and R_{15} modes, and compare the energies of this structure and structures distorted in the eigenvectors of the ferroelectric Γ_{15} mode and the R_{15} mode at the Brillouin zone boundary. Finally, in Conclusions, we briefly formulate the main results of this work.

2. LATTICE DYNAMICS

The calculation is performed in terms of the generalized Gordon–Kim model with allowance for dipole and quadrupole ion polarizabilities [13]. We only consider fully disordered solid solutions with a perovskite structure (space group $Pm3m$). To calculate a disordered solid solution, we used the virtual crystal approximation [14]. The unit cell parameters were determined through minimization of the total crystal energy, and they are given in Table 1 along with the well-known experimental values.

The calculated unit cell parameters are seen to be 1–3% smaller than the experimental values. The ferroelectric instability is known to be extremely sensitive to the unit cell volume [18]; therefore, the lattice dynamics and the energies of the low-symmetry phases were calculated using the experimental values of the lattice parameters. For crystals with B' = Ga and Lu (for which the experimental values of the lattice parameters are unknown), the calculation was carried out at the following lattice parameters: this parameter was taken to be 4.07 Å for the gallium compounds, 4.13 Å for PLT, and 4.15 Å for PLN.

With this model, we calculated the rf permittivity, dynamic Born charges, elastic constants (Table 2), and lattice vibration frequency spectra of disordered $PbGa_{1/2}Nb_{1/2}O_3$ (PGN), $PbGa_{1/2}Ta_{1/2}O_3$ (PGT), PIN, PIT, PLN, and PLT solid solutions. As is seen in Table 2, the dynamic charges of the $\langle B\rangle$ and $O_\perp$ ions decrease with increasing atomic number of the $\langle B\rangle$ ion. This tendency was also noted in [11]. Table 3 gives the vibration frequencies at the center of the Brillouin zone and at boundary point R ($q = 2\pi/a(1/2, 1/2, 1/2)$. Here, we do not present complete phonon spectra, since they are qualitatively similar in all these compounds (the spectra for PSN and PST are given in [11]). Crystals of the entire series $PbB'_{1/2}B''_{1/2}O_3$ exhibit a soft vibrational mode with symmetry Γ_{15}, which corresponds to the ferroelectric instability of the lattice, at the center of the Brillouin zone. As to the nature of the ferroelectric phase transition in oxides with a perovskite structure, there are two viewpoints: some researchers believe that this transition is an order–disorder transition [19] and is related to the ordering of the B ion occupying the central position in the octahedron, and other researchers attribute this transition to displacive phase transitions and relate it to lattice instability with respect to a trans-

Table 2. Calculated rf permittivity ε_∞, dynamic Born charges Z^{din}, elastic constants C_{ij}, short-range dipole–charge interaction $T_{\langle B\rangle-O}$, cell polarizability α_{cell}, C_0/C_1 ratio, and soft ferroelectric mode frequency ω_s

	ε_∞	Z^{din}_{Pb}	$Z^{din}_{\langle B\rangle}$	$Z^{din}_{O\parallel}$	$Z^{din}_{O\perp}$	C_{11}, 10^2 GPa	C_{12}, 10^2 GPa	C_{44}, 10^2 GPa	$T_{\langle B\rangle-O}$, a. u.	α_{cell}, a. u.	$-C_0/C_1$, $4\pi e^2/V$	ω_s, cm^{-1}
PSN	3.57	2.70	5.17	–4.19	–1.84	1.58	0.72	0.82	0.220	49.7	–0.53	–75
PGN	3.00	2.67	4.55	–3.23	–2.00	2.23	0.75	0.90	0.235	43.5	–0.41	–66
PIN	3.02	2.70	4.60	–3.08	–2.10	1.77	0.66	0.77	0.251	44.6	–0.52	–71
PLN	2.80	2.64	4.20	–2.53	–2.16	1.80	0.60	0.70	0.255	43.1	–0.57	–72
PST	3.35	2.66	4.27	–2.86	–2.04	2.09	0.74	0.75	0.260	47.6	–0.26	–53
PGT	2.90	2.64	3.94	–2.32	–2.13	2.12	0.73	0.83	0.270	42.3	–0.35	–60
PIT	2.94	2.66	2.96	–2.2	–2.22	2.27	0.68	0.72	0.280	43.3	–0.51	–70
PLT	2.74	2.62	3.62	–1.65	–2.30	2.40	0.65	0.68	0.290	41.8	–0.64	–76

Table 3. Vibration frequencies (cm^{-1}) at $q = 0$ and $q = R$ for disordered $PbB'_{1/2}B''_{1/2}O_3$ solid solutions

	PSN	PGN	PIN	PLN	PST	PGT	PIT	PLT
				$q = 0$				
$\Gamma_{15}(2)$ TO	–75.1	–53.1	–71.4	–71.8	–53.5	–56.8	–70.5	–75.7
$\Gamma_{25}(1)$ LO	83.8	107.8	96.6	98.2	101.8	111.3	103.7	100.5
$T_{2u}(3)$	164.9	220.4	206.7	198.1	196.3	207.2	189.9	179.6
$T_{1u}(2)$ TO	201.3	252.1	251.6	242.2	230.5	250.8	240.2	231.7
$T_{1u}(1)$ LO	330.9	362.1	352.8	360.7	337.6	389.0	359.4	369.8
$T_{1u}(2)$ TO	338.7	412.4	417.9	477.9	488.8	511.7	522.9	545.8
$T_{1u}(1)$ LO	480.2	524.4	520.8	540.4	550.8	560.0	568.0	570.4
				$q = R$				
$R_{15}(3)$	–52.6	–49.4	–61.8	–63.6	–54.2	–53.9	–62.8	–66.7
$R_{25}(3)$	81.6	93.7	–16.1	–61.1	–38.8	–47.0	–105.0	–127.4
$R_{15}(3)$	243.2	266.6	254.5	228.5	222.2	245.5	229.8	212.9
$R_{25'}(3)$	250.2	287.8	270.7	268.7	255.1	267.3	265.9	266.3
$R_{12'}(2)$	296.5	347.2	401.9	440.9	441.9	460.6	497.8	515.7
$R_{2'}(1)$	576.1	596.0	571.1	578.4	604.1	591.8	590.3	578.5

Note: In parentheses, mode degeneracy is given, and soft modes are indicated by negative values.

verse optical mode. In the case of a displacive phase transition, it was found that the ferroelectric instability in oxides with a perovskite structure is specified by a fine balance between competing long-range dipole–dipole and short-range interactions. As was shown in [11], the magnitude and sign of the ferroelectric mode frequency are determined by virtually all interactions in a crystal, and a key role is played by the competition between long-range dipole–dipole interactions and the short-range interactions between the B ion charge and the electron dipole moment of oxygen in the $B–O_{\parallel}$ bond. This competition also substantially affects the Born charge at the B and $O_{\parallel}$ ions. Table 2 (column 9) gives the calculated values of the short-range charge–dipole $T_{\langle B\rangle-O_{\parallel}}$ interaction, and column 10 gives the values of cell polarizability α_{cell} [20], which depends on the polarizabilities of the cell ions and, thus, characterizes the dipole–dipole interaction to a certain extent. A comparison of these values for different compounds demonstrates that, if the ferroelectric instability were determined by only these interactions, PLT should be the most "rigid" among the compounds and PSN should be the "softest." However, the ferroelectric mode frequencies in these compounds are the same. This finding again supports the conclusion in [11] regarding the fact that all interactions in a crystal contribute to the ferroelectric instability in these compounds. In [11], we showed that the soft ferroelectric mode frequency in a perovskite structure can be approximately written as

$$\omega^2 \approx -C_0/C_1, \quad (1)$$

where C_0 and C_1 are the combinations of the dynamic matrix elements in the designations of [11]. The last two columns in Table 2 present the calculated values of the C_0/C_1 ratio and the soft ferroelectric mode frequency. It is seen that C_0/C_1 changes weakly (from –0.65 to –0.25) for the entire series of compounds and that, correspondingly, the unstable ferroelectric vibration frequencies for all compounds are approximately the same. Therefore, although the presence of ferroelectric instability is mainly determined by the competition of long-range dipole–dipole and short-range dipole–charge $T_{B–O}$ interactions, the soft mode frequency is controlled by a finer balance between all interactions in a crystal [11].

3. FERROELECTRIC INSTABILITY AND THE FERROELECTRIC PHASE TRANSITION

The ferroelectric instability in lead-containing solid solutions is mainly related to the displacement of the lead and oxygen ions in the direction normal to the ⟨B⟩–O bond [18]. Table 4 lists the calculated eigenvectors of the unstable ferroelectric modes in the series of the compounds under study. The Pb and $O_{\perp}$ ions are seen to exhibit the maximum displacements, and these are virtually the same for all compounds.

When a crystal is distorted along the eigenvector of the soft ferroelectric mode, a structure with ions displaced along the spatial diagonal of the cubic cell, which corresponds to the symmetry of the rhombohedral phase, turns out to be energetically favorable. Figure 1 shows the dependences of the crystal energy cal-

Table 4. Eigenvectors of soft ferroelectric mode Γ_{15}

	Pb	⟨B⟩	$O_\perp$	$O_\parallel$
PSN	0.76	0.21	−0.42	−0.14
PST	0.77	0.11	−0.44	−0.01
PGN	0.78	0.12	−0.43	−0.05
PGT	0.78	0.08	−0.44	−0.02
PIN	0.79	0.08	−0.42	−0.03
PIT	0.78	0.07	−0.44	−0.02
PLN	0.79	0.06	−0.43	−0.004
PLT	0.79	0.06	−0.43	−0.02

culated with respect to the energy of the undistorted cubic crystal ($E_\Gamma - E_0$) on the ion displacement amplitude along the eigenvector of the soft ferroelectric mode in the [111] direction. The energy minimum depth increases with the atomic number of ion B' and shifts toward large ion displacement amplitudes from the equilibrium position in the cubic phase. The ferroelectric phase transition temperatures were calculated with a model Hamiltonian in the local mode approximation [12, 21–23]. The three-component local mode

$$S^\alpha = u^\alpha \sum_i \xi_{i\alpha},$$

where **u** is the ion displacement amplitude and $\xi_{k\alpha}$ is the eigenvector of the mode from Table 4, was centered at the Pb ions, which undergo the maximum displacement, and was located on the sites of the simple cubic lattice. The model Hamiltonian included the energies of the short-range interactions within three coordination shells (E_{short}), the long-range dipole–dipole interactions

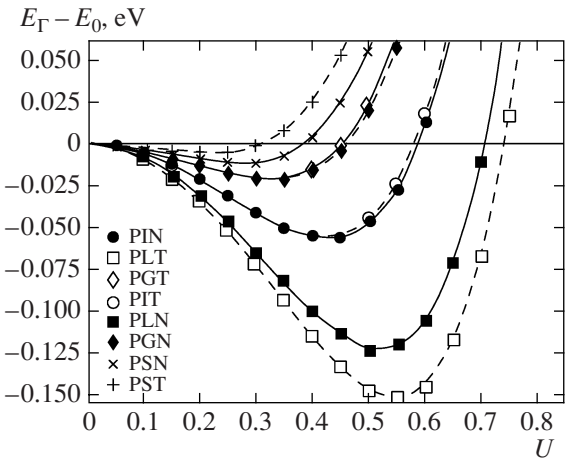

Fig. 1. Dependences of the total energies of $PbB'_{1/2}B''_{1/2}O_3$ solid solutions on the amplitude of ion displacements in the eigenvector of the ferroelectric mode in the [111] direction.

of local modes (E_{dip}), and single-site anharmonicity (E_{anhar}),

$$E^{\text{tot}} = E^{\text{anhar}}(\{\mathbf{S}_i\}) + E^{\text{short}}(\{\mathbf{S}_i\}, \{\mathbf{S}_j\}) + E^{\text{dip}}(\{\mathbf{S}_i\}, \{\mathbf{S}_j\}). \quad (2)$$

An explicit expression for the model Hamiltonian and the procedure of the determination of the Hamiltonian parameters from a set of the energies of distorted structures were given in [22]. Table 5 presents the model Hamiltonian parameters calculated for all solid solutions.

The temperature behavior of the system with model Hamiltonian (2) was calculated by the Monte Carlo method with the parameters taken from Table 5. The Monte Carlo procedure was described in [12], where the ferroelectric phase transition in PSN and PST compounds was calculated. The results of the Monte Carlo calculation demonstrate that all fully disordered solid solutions except for PSN undergo a phase transition into the rhombohedral ferroelectric phase with approximately the same nonzero values of three local-mode components. In the PSN solid solution, the Monte Carlo procedure reveals a narrow intermediate temperature range of the ferroelectric phase with two nonzero and the same local-mode components [12]. The temperature dependence of the internal energy of the system is virtually smooth; however, the temperature dependences of the contributions to the energy (short-range and dipole–dipole energies) contain noticeable inflection points in the phase transition region, which were used to determine the phase transition temperatures. The temperature dependences of the energy and its contributions calculated by the Monte Carlo method for PSN and PST are given in [12]. Similar dependences are observed in other compounds of the series of solid solutions, and we do not present them here to save space. In Table 5, we give the temperatures of the phase transition from the cubic into the rhombohedral ferroelectric phase and the spontaneous polarization of the latter phase that were calculated by the Monte Carlo method. In Fig. 2, we show the temperature dependences of the spontaneous polarization in the ferroelectric phase. As is seen in Fig. 2, the inflection points in the temperature dependences of the spontaneous polarization approximately coincide with the phase transition temperatures determined from the temperature dependences of the energy (Table 5). Although the model Hamiltonian parameters for different compositions are rather close to each other (see Table 5), the scatter of the transition temperatures is rather large, from 170 to 850 K. As follows from Table 5, the ferroelectric-transition temperature increases with the atomic number of ion B' in both the niobium and tantalum compounds, with the ferroelectric phase in the tantalum $PbB'_{1/2}Ta_{1/2}O_3$ solid solutions stabilizing at higher temperatures than in $PbB'_{1/2}Nb_{1/2}O_3$ except for

Table 5. Model Hamiltonian parameters

	PSN	PGN	PIN	PLN	PST	PGT	PIT	PLT
j_1, eV	–35.5	–25.6	–24.6	–24.8	–23.0	–23.0	–15.0	–24.6
j_2, eV	92.2	59.7	60.7	60	41.7	41.7	46.2	63.0
j_3, eV	12.2	8.1	7.9	7.7	7.2	7.2	11.7	8.6
j_4, eV	–8.0	–6.7	–5.1	–5.0	–11.6	–11.6	–10.2	–4.8
j_5, eV	24.2	21.4	9.03	9.4	16.4	16.4	21.8	26.0
j_6, eV	3.3	2.8	2.1	2.2	5.3	5.3	1.4	2.7
j_7, eV	1.6	1.4	1.1	1.0	2.6	2.6	1.2	1.3
A, eV	40	40.5	34.5	35.6	51	51	33.6	15.7
B, eV	1176	1247	1110	1136	1193	1193	1234	1302
C, eV	1350	2239	1883	1652	1602	1602	1940	1620
Z	5.28	5.20	4.40	4.22	4.31	4.33	4.21	4.25
T_c, K (calculation)	250	280	380	630	170	650	800	850
T_c, K (experiment)	380 [24]	–	325 [10]	–	275 [24]	–	425 [10]	–
P_s, C/m^2 (calculation)	0.26	0.2	0.28	0.37	0.17	0.34	0.39	0.41
P_s, C/m^2 (experiment)	–	–	0.14 [25]	–	0.33 [17]	–	–	–
E_{dip}, eV	–0.25	–0.41	–0.63	–0.90	–0.16	–0.40	–0.63	–0.71

Note: j_1–j_7 stand for short-range interaction parameters; A, B, and C, for single-site anharmonicity parameters; Z, effective mode charge; T_c, ferroelectric phase transition temperature; P_s, spontaneous polarization; and E_{dip}, dipole–dipole interaction energy.

PSN and PST (where the converse situation takes place). Correspondingly, the spontaneous polarization in the tantalates is higher than in the niobates. Dipole–dipole interactions still are still the most important forces stabilizing the ferroelectric phase. The stronger these interactions, the higher the ferroelectric phase temperature and the higher the ferroelectric phase transition temperature. Table 5 lists the dipole energies for the compounds under study that were calculated at the amplitude corresponding to the minimum energy for the ion displacements in the [111] direction (Fig. 1). It is seen that higher dipole energies correspond to higher phase transition temperatures in the series of both tantalates and niobates. An increase in the dipole–dipole interaction energy is related to higher displacement amplitudes for compounds with larger atomic numbers of ion B'. The cause of the fact that the transition temperatures in the tantalates are higher than in the niobates (except for PSN and PST) is still unclear. It should be noted that the tendency toward an increase in the ferroelectric phase transition temperature with the atomic number of ion B' is also experimentally detected and that this tendency in our calculations is more pronounced.

4. ANTIFERROELECTRIC INSTABILITY

As was noted in the Introduction, the experimental studies of $PbB'_{1/2}Nb_{1/2}O_3$ and $PbB'_{1/2}Ta_{1/2}O_3$, where B' = Ga, In, and Lu, are few, and they are most completely reviewed in [10]. According to certain experimental data, the low-temperature phase is ferroelectric in solid solutions with In and Lu used as ion B' at a certain degree of ordering of B cations. The symmetry of this phase has not been reliably established: according to [10, 26], this is a rhombohedral phase for PIN; according to [1, 8], this is an orthorhombic phase with space group *Pbam*, as in $PbZrO_3$.

When the structures of the antiferroelectric phases in compounds such as $PbIn_{1/2}Nb_{1/2}O_3$ or Pb_2MgWO_6 [27] were studied, researchers, as a rule, used an analogy with the structure of the antiferroelectric phase in

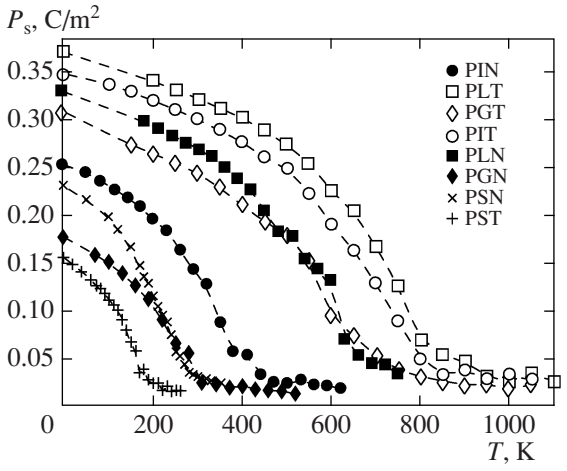

Fig. 2. Temperature dependences of the spontaneous polarizations of $PbB'_{1/2}B''_{1/2}O_3$ solid solutions.

Table 6. Eigenvectors of mode R_{15}

	PSN	PST	PGN	PGT	PIN	PIT	PLN	PLT
Pb	0.65	0.65	0.67	0.67	0.71	0.70	0.72	0.70
O	0.53	0.53	0.52	0.52	0.50	0.51	0.49	0.50

$PbZrO_3$, which is considered to be a classic antiferroelectric. According to the symmetry analysis performed in [28], the antiferroelectric structure in $PbZrO_3$ can result from the quenching of the vibration modes of the cubic lattice that belong to several wavevectors in the Brillouin zone, namely, at the center of the zone, at its boundary points M and R, and along the $\Gamma \longrightarrow M$ direction. As a result, a rather complex structure can form. However, as follows from the structural studies of the antiferroelectric phases in lead-containing oxides [1, 5, 10], the main characteristic feature of these structures consists in an antiparallel Pb ion displacements and weak distortions in the oxygen octahedra.

The phonon spectra calculated for all solid solutions contain a triply degenerate metastable lattice vibration mode with symmetry R_{15} at point R in the Brillouin zone boundary. The lead and oxygen ions shift in the eigenvector of this mode as follows [29]:

$$\begin{gathered} \mathrm{Pb}_x, \mathrm{O}_{\mathrm{I}y} = \mathrm{O}_{\mathrm{II}z}; \mathrm{Pb}_y, \quad \mathrm{O}_{\mathrm{I}x} = \mathrm{O}_{\mathrm{III}z}; \\ \mathrm{Pb}_z, \mathrm{O}_{\mathrm{II}x} = \mathrm{O}_{\mathrm{III}y}. \end{gathered} \tag{3}$$

Table 6 lists the eigenvectors of this mode calculated for the entire series of the solid solutions, including PSN and PST.

The frequencies of the soft R_{15} modes in all compounds are close to each other and to the frequencies of the soft ferroelectric modes (see Table 3). Nevertheless, the instability mechanisms of these two modes are different. The main cause of the instability of polar ferroelectric mode Γ_{15} is represented by dipole–dipole forces, whereas dipole–charge interactions stabilize the ferroelectric mode. Our calculations demonstrate that, in mode R_{15} at the Brillouin zone boundary, the dipole–charge (both long- and short-range) interactions play a destabilizing role and soften this mode.

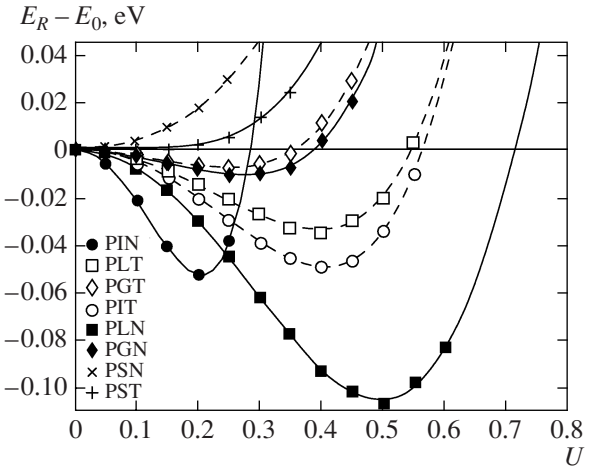

Fig. 3. Dependences of the total energies of $PbB'_{1/2}B''_{1/2}O_3$ solid solutions on the amplitude of ion displacements in the eigenvector of mode R_{15} in the [111] direction.

When ions shift along the eigenvectors of soft mode $R_{15}(3)$, the perovskite unit cell doubles (elpasolite structure), with Pb displacements being antiparallel in neighboring cells. The displacements of the Pb and O ions along all three vectors (3) turn out to be energetically favorable; the dependence of the total energy E_R–E_0 on the ion displacement amplitude is shown in Fig. 3. It is seen that the lattice distortions in the eigenvectors of soft mode R_{15} are energetically favorable compared to a cubic structure for all compounds except for PSN, and this energy gain for PST is very small. The energies of all structures except for PSN and PST with ferroelectric distortions and with distortions in the eigenvector of unstable mode R_{15} in solid solutions are close (Table 7; Figs. 1, 3).

Thus, our calculations demonstrate that $PbB'_{1/2}B''_{1/2}O_3$ (B' = Sc, Ga, In, Lu; B" = Nb, Ta) solid solutions have two strongly unstable lattice vibration modes, namely, ferroelectric mode Γ_{15} at the center of the Brillouin zone and mode R_{15} at the Brillouin zone boundary. In both unstable modes, Pb and O ion displacements are predominant, and the energies of the structures distorted in the eigenvectors of these modes are close.

Based on these results, we can propose a simple model for the antiferroelectric state in the solid solutions under study. In this model, soft mode R_{15} (which causes unit cell doubling and antiparallel atomic displacements in neighboring cells) "entrains" the polar ferroelectric mode; as a consequence, the resulting state of the crystal becomes antiferroelectric (Fig. 4). Figure 4 shows two possible situations of the condensation of these modes: the atomic displacements that correspond to mode Γ_{15} are antiparallel (Fig. 4a) or parallel (Fig. 4b) in neighboring unit cells. For simplicity, we show atomic displacements only in the [001] direction. According to our calculations, the situation where the atomic displacements in the eigenvector of the ferroelectric mode occur in the [111] direction and are antiparallel in neighboring cells is energetically favorable (Table 7). In the case of parallel atomic displacements in neighboring cells, an energy gain in the distorted structure appears only at certain amplitudes (approximately 0.2) of atomic displacements in the eigenvector of mode R_{15} and at sufficiently low amplitudes (0.05) of atomic displacements in the eigenvector of the ferroelectric mode. Thus, an antiferroelectric state in this model can be generated via the distortion of the structure in the eigenvectors of modes R_{15} and Γ_{15} with antiparallel atomic displacements in neighboring cells. Figure 5 shows the dependence of the total energy $E_{R\Gamma\uparrow\downarrow} - E_0$ on the amplitude of the ion displacements

Table 7. Energies of distorted structures obtained when atoms shift in the eigenvectors of modes Γ_{15} ($q = 0$) and R_{15} ($q = 2\pi/a(1/2, 1/2, 1/2)$)

	$E_\Gamma - E_0$, eV	$E_R - E_0$, eV	$E_{R\Gamma\uparrow\downarrow} - E_0$, eV	$E_{R\Gamma\uparrow\uparrow} - E_0$, eV	Δ, eV
PSN	−0.0110	+0.0005	+0.0145	+0.0200	2.312
PGN	−0.0220	−0.0080	−0.0087	−0.0014	0.604
PIN	−0.0560	−0.0500	−0.0480	−0.0410	0.142
PLN	−0.1230	−0.0340	−0.0780	−0.012	0.365
PST	−0.0050	−0.0004	+0.0140	+0.0180	3.8
PGT	−0.0210	−0.0110	−0.0100	−0.0030	0.5
PIT	−0.0550	−0.0520	−0.0570	−0.0430	0.036
PLT	−0.1510	−0.1060	−0.1200	−0.0940	0.2

Note: E_Γ stands for the energy of the structure distorted only in the vector of ferroelectric mode Γ_{15}; E_R, for the energy of the structure distorted only in the vector of mode R_{15}; $E_{R\Gamma\uparrow\downarrow}$, the energy of the model antiferroelectric structure distorted in the vectors of modes Γ_{15} and R_{15} with antiparallel atomic displacements in the eigenvector of ferroelectric mode Γ_{15} in neighboring cells; $E_{R\Gamma\uparrow\uparrow}$, the same but with parallel atomic displacements in neighboring cells; and Δ, the relative difference between the energies of the ferroelectric and "antiferroelectric" phases.

corresponding to the condensation of these two modes. The abscissa is the amplitude of atomic displacements in the eigenvector of the ferroelectric mode, and the amplitude of atomic displacements in the eigenvector of mode R_{15} was taken to be such that the total structural distortion was energetically favorable. The model antiferroelectric state obtained is seen to be energetically favorable compared to a cubic structure for all compounds of the series except for PSN and PST. As the atomic number of ion B' increases, the depth of the minimum increases and shifts toward high displacement amplitudes from the equilibrium position in the cubic phase. As follows from Table 7, the energy of the antiferroelectric distorted structure for the indium and lutecium compounds, in contrast to the scandium and gallium compounds, turns out to be approximately equal to the energies of the structures distorted only in the eigenvector of mode R_{15} or Γ_{15} and to remain ener-

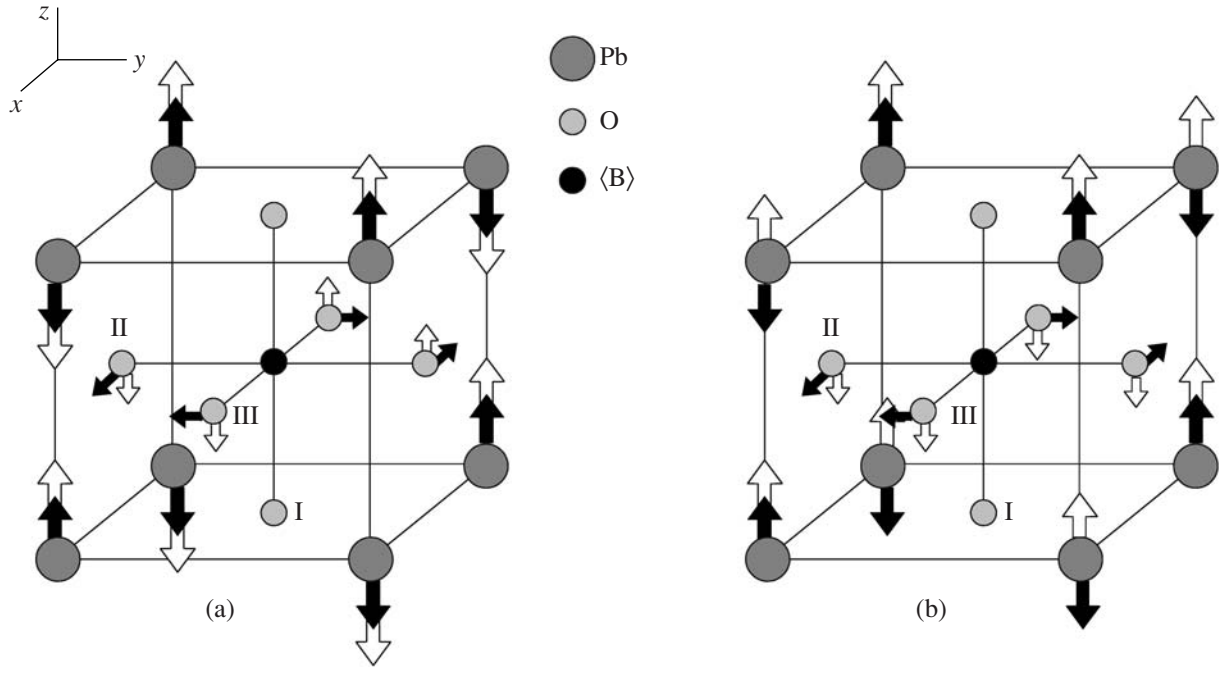

Fig. 4. Possible condensation of mode R_{15} and ferroelectric mode Γ_{15} with (a) antiparallel and (b) parallel displacements in neighboring cells. Solid arrows indicate the direction of atomic displacements corresponding to mode R_{15}, and open arrows indicate the direction of atomic displacements corresponding to the ferroelectric mode. The designations of oxygen are given in accordance with [29].

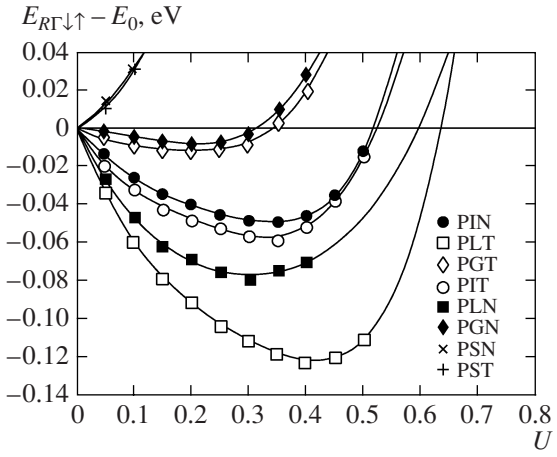

Fig. 5. Dependence of the total energy of the model antiferroelectric structure of $PbB'_{1/2}B''_{1/2}O_3$ solid solutions (Fig. 4a) on the amplitude U of ion displacements in the eigenvectors of modes Γ_{15} and R_{15} in the [111] direction. The amplitude of displacements in the eigenvector of mode R_{15} was taken to be 0.05 for the scandium compounds, 0.1 for the gallium compounds, 0.2 for the indium compounds, and 0.25 for the lutecium compounds.

getically less favorable compared to these structures except for PIT (in which the model antiferroelectric state turns out to be energetically more favorable). The last column in Table 7 gives the relative difference in the energies of the ferroelectric and "antiferroelectric" phases ($\Delta = ((E_{R\Gamma\uparrow\downarrow} - E_0) - (E_\Gamma - E_0))/(E_\Gamma - E_0)$). This difference is maximal in the compounds with scandium and decreases with increasing the atomic number of cation B'. However, the dependence of the difference in the energies of the two phases on the atomic number of cation B' is nonmonotonic: this difference is minimal in the compounds with indium. These theoretical results are qualitatively supported by available experimental data, according to which an antiferroelectric phase was detected in the PIN compound and was assumed to be present in PLT and PLN. Thus, we may conclude that a phase transition into an antiferroelectric phase can exist in these compounds; therefore, it is desirable to have experimental evidence for the presence of this phase.

5. CONCLUSIONS

(1) The calculated lattice vibration spectra of disordered $PbB'_{1/2}B''_{1/2}O_3$ (B' = Ga, In, Lu; B" = Nb, Ta) solid solutions with a perovskite structure have unstable modes that are responsible for lattice instability with respect to polar vibrations (mode Γ_{15}) and to vibrations with a wavevector located at the Brillouin zone boundary (mode R_{15}). The frequencies of these modes are close. The lead ions shift mainly in the eigenvectors of these modes.

(2) Using the local mode approximation, we determined the parameters of the effective Hamiltonian that describes a ferroelectric phase transition and calculated the temperatures of this transition for all the solid solutions under study. We found that these temperatures for the tantalum compounds are higher than for the niobium compounds and that the transition temperature increases with the atomic number of ion B' in the compounds. The same dependence was obtained for the calculated spontaneous polarization.

(3) We considered the possibility of an antiferroelectric state in the compounds under study. The structure of the antiferroelectric phase represents a combination of ion displacements in the eigenvectors of mode R_{15} and polar mode Γ_{15}, and the displacements in the eigenvector of the polar mode are opposite in neighboring cells of a perovskite structure. This phase, the ferroelectric phase, and the phase related to the condensation of only mode R_{15} are found to have similar energies for all compounds except for $PbSc_{1/2}Ta_{1/2}O_3$ and $PbSc_{1/2}Nb_{1/2}O_3$. In the $PbIn_{1/2}Ta_{1/2}O_3$ compound, the antiferroelectric phase turns out to be energetically more favorable than the ferroelectric phase and the phase related to the condensation of mode R_{15}.

ACKNOWLEDGMENTS

This work was supported by the Russian Foundation for Basic Research (project no. 06-02-16091) and the Presidential Program of Support for Leading Scientific Schools in Russia (project no. NSh-4137.2006.2).

REFERENCES

1. Y. Park, K. M. Knowles, and K. Cho, Phase Transitions **68**, 411 (1999).
2. P. M. Woodward and K. Z. Baba-Kishi, J. Appl. Crystallogr. **35**, 233 (2002).
3. K. Z. Baba-Kishi, G. Kressey, and R. J. Cernic, J. Appl. Crystallogr. **25**, 477 (1992).
4. *Ferroelectrics and Antiferroelectrics*, Ed. by G. A. Smolenskiĭ (Nauka, Moscow, 1971) [in Russian].
5. K. Nomura, T. Shingai, N. Yasuda, et al., Ferroelectrics **218**, 69 (1998).
6. A. A. Bokov, I. P. Rayevsky, V. V. Neprin, and V. G. Smotrakov, Ferroelectrics **124**, 271 (1991).
7. V. A. Shuvaeva, Y. Azuma, I. P. Raevski, et al., Ferroelectrics **299**, 103 (2004).
8. P. Groves, Phase Transitions **6**, 115 (1986).
9. P. Groves, J. Phys. C: Solid State Phys. **19**, 5103 (1986).
10. V. A. Isupov, Ferroelectrics **289**, 131 (2003).
11. V. I. Zinenko, N. G. Zamkova, E. G. Maksimov, and S. N. Sofronova, Zh. Éksp. Teor. Fiz. **132** (3), 702 (2007) [JETP **105** (3), 617 (2007)].
12. V. I. Zinenko and N. G. Zamkova, Zh. Éksp. Teor. Fiz. **133** (3), 622 (2008) [JETP **106** (3), 542 (2008)].
13. E. G. Maksimov, V. I. Zinenko, and N. G. Zamkova, Usp. Fiz. Nauk **174** (11), 1145 (2004) [Phys.—Usp. **47** (11), 1075 (2004)].

14. V. I. Zinenko and S. N. Sofronova, Fiz. Tverd. Tela (St. Petersburg) **46** (7), 1252 (2004) [Phys. Solid State **46** (7), 1291 (2004)].
15. C. Perrin, N. Menguy, O. Bidault, et al., J. Phys.: Condens. Matter **13**, 10231 (2001).
16. C. G. F. Stenger and A. J. Burggraaf, Phys. Status Solidi A **61**, 275 (1980).
17. A. Kania and N. Pavlaczyk, Ferroelectrics **124**, 261 (1991).
18. W. Zhong, R. D. King-Smith, and D. Vanderbilt, Phys Rev. Lett. **72**, 3618 (1994).
19. G. Volkel and K. A. Muller, Phys. Rev. B: Condens. Matter **76**, 094105 (2007).
20. O. V. Ivanov, D. A. Shport, and E. G. Maksimov, Zh. Éksp. Teor. Fiz. **114** (1), 333 (1998) [JETP **87** (1), 186 (1998)].
21. U. V. Waghmare and K. M. Rabe, Phys. Rev. B: Condens. Matter **55**, 6161 (1997).
22. W. Zhong and D. Vanderbilt, Phys. Rev. B: Condens. Matter **52**, 6301 (1995).
23. K. M. Rabe and J. D. Jannopoulos, Phys. Rev. B: Condens. Matter **36**, 6631 (1987).
24. C. Malibert, B. Dkhil, J. M. Kiat, et al., J. Phys.: Condens. Matter **9**, 7485 (1997).
25. S. Wongsaenmai, R. Yimnirun, S. Ananta, et al., Mater. Lett. **62**, 352 (2007).
26. M. F. Kuprianov, A. V. Turik, S. M. Zaitsev, and E. G. Fesenko, Phase Transitions **4**, 65 (1983).
27. G. Baldinozzi, Ph. Sciau, D. Grebillet, et al., Acta Crystallogr., Sect. B: Struct. Sci. **51**, 668 (1995).
28. W. Cohran and A. Zia, Phys. Status Solidi **25**, 273 (1968).
29. R. F. Cowley, Phys. Rev. **134**, A981 (1964).

Translated by K. Shakhlevich